Nanosize effect on the hygroscopic growth factor of aerosol particles

G. Biskos,[1] L. M. Russell,[2] P. R. Buseck,[3] and S. T. Martin[1]

Received 10 November 2005; revised 16 January 2006; accepted 23 February 2006; published 1 April 2006.

[1] The hygroscopic growth factors of NaCl particles having dry mobility diameters of 6 to 60 nm were measured using a tandem nano-Differential Mobility Analyzer. The growth factors steadily decreased within detection limit for dry sizes below 40 nm. The decrease is quantitatively predicted by a model that includes the Kelvin effect and a size-dependent shape factor. This factor is not tuned to the data but rather is grounded in theoretical predictions from literature. Agreement in growth factors for particles generated by two independent methods (namely, vaporization-condensation and electrospray), as well as observations of prompt deliquescence, indicates the absence of significant chemical impurities. **Citation:** Biskos, G., L. M. Russell, P. R. Buseck, and S. T. Martin (2006), Nanosize effect on the hygroscopic growth factor of aerosol particles, *Geophys. Res. Lett.*, *33*, L07801, doi:10.1029/2005GL025199.

1. Introduction

[2] Atmospheric nanoparticles include ammonium sulfate [*Zhang et al.*, 2004], iodine oxides [*O'Dowd et al.*, 2002a], secondary organic aerosol [*O'Dowd et al.*, 2002b], and sea salt [*Clarke et al.*, 2003]. By processes of coagulation and condensational growth, atmospheric nanoparticles are important precursors to the accumulation-mode particles that influence cloud formation [*Russell et al.*, 1999; *Anastasio and Martin*, 2001]. The aerodynamic diameter of hygroscopic particles, which partially determines the rates of coagulation and condensation, depends on relative humidity [*Tang et al.*, 1997]. For nanoparticles, the hygroscopic growth factor at a fixed relative humidity is predicted to decrease with smaller sizes because of the Kelvin effect [*Chen*, 1994].

[3] A further nanosize effect on hygroscopic growth, beyond the Kelvin correction, could also result from a dependency of a particle property on size. For instance, as particle size decreases below a threshold, surface tension decreases due to the increased curvature. A typical estimated threshold is 2 nm as the particle size approaches bond distances [*Lu and Jiang*, 2005], although the relationship has not been tested experimentally and could begin at larger sizes. Density increases by approximately 1% below a critical size of 1 to 5 nm for typical materials [*Cheng et al.*, 1993; *Gilbert et al.*, 2004]. The shape factor of nonspherical particles is expected to become size dependent when the Knudsen number (given by $2\lambda/d$) lies in the transition regime of $0.1 < \mathrm{Kn} < 10$, where λ is the mean free path of a gas molecule 66 nm in 1 atm of air) and d is particle size [*DeCarlo et al.*, 2004]. Nonspherical particles have a shape factor to account for the difference in drag force compared to a spherical particle.

[4] In addition to nanosize effects on intrinsic particle properties, predictions of hygroscopic growth have increased sensitivity in the nanosize regime to parameter uncertainties. Figure 1b shows a sensitivity of 1 to 10% in the predicted hygroscopic growth of NaCl particles for potential uncertainties in aqueous-particle surface tension, dry-particle density, and dry-particle shape factor. The impacts of the uncertainties are greatest for nanoparticles.

[5] Despite their possible importance, experimental investigations of nanosize effects are few, and related results in these previous studies of prompt and nonprompt deliquescence and efflorescence are difficult to rationalize [*Hämeri et al.*, 2000, 2001; *Djikaev et al.*, 2001]. Contamination of the nanoparticles may have affected the results. *Biskos et al.* [2006] recently reported prompt deliquescence and efflorescence for nanoparticles believed to have low levels of impurities.

[6] In this paper, we report new measurements of the hygroscopic growth of nanoparticles and evaluate how well existing models predict the observations. The test system is 6- to 60-nm NaCl aerosol particles. The inorganic composition of desiccated sea water is 86 wt% NaCl. Based upon the discussion above for size dependencies of properties, the test aerosol particles may be expected to have large-particle values of aqueous-gas surface tension and aqueous-/dry-particle densities. A size dependency in the dry-particle shape factor, however, may be expected.

2. Theory of the Nanosize Effect on the Hygroscopic Growth Factor

[7] The observable of our experimental method is particle mobility diameter d_m. The mobility-diameter growth factor g is given by:

$$g(\mathrm{RH}) = \frac{d_m(\mathrm{RH})}{d_{m,dry}}, \quad (1)$$

where $d_{m,dry}$ is the mobility diameter of the dry particle (viz. RH < 5%) and d_m(RH) is the mobility diameter at increased relative humidity (RH).

[8] The growth factor can be predicted by equation (1) when the relationship between d_m(RH) and $d_{m,dry}$ is known or modeled. We consider four models. In each, we assume that NaCl deliquesces at the RH of d_m(RH) so that a spherical (i.e., unity shape factor) aqueous particle forms. As a result, d_m(RH) = d_{ve}(RH) where d_{ve} is the volume-equivalent (i.e., spherical) diameter.

[1]Division of Engineering and Applied Sciences, Harvard University, Cambridge, Massachusetts, USA.
[2]Scripps Institution of Oceanography, University of California, San Diego, La Jolla, California, USA.
[3]Departments of Geological Sciences and Chemistry/Biochemistry, Arizona State University, Tempe, Arizona, USA.

0094-8276/06/2005GL025199$05.00

[9] Model 1 assumes that the shape factor of the dry particle is unity. In this case, $d_{m,dry} = d_{ve,dry}$. We obtain:

$$d_{ve}(\mathrm{RH}) \equiv \left(\frac{100\rho_s}{w_t(a_w)\rho(w_t(a_w))}\right)^{1/3} d_{ve,dry} \tag{2a}$$

$$= \left(\frac{100\rho_s}{w_t(a_w)\rho(w_t(a_w))}\right)^{1/3} d_{m,dry}, \tag{2b}$$

where ρ_s is the density of the dry particle, $\rho(w_t)$ is the density of the aqueous solution droplet, and w_t is the weight percent of solute in the aqueous particle. Weight percent composition depends on water activity a_w. Equations for all quantities for NaCl are given in Table S1[1]. Model 1 also assumes that a_w = RH/100, thus omitting the Kelvin effect. The growth factor for this model is then calculated by equations (1) and (2b).

[10] Model 2 expands on model 1 by including the Kelvin effect, which relates RH to a_w as follows:

$$\mathrm{RH} = 100 a_w \exp\left(\frac{4M_w\sigma_{aq}(w_t(a_w))}{RT\rho_w d_{ve}(\mathrm{RH})}\right), \tag{3}$$

where ρ_w is the density of water, σ_{aq} is the surface tension of the aqueous droplet (Table S1), M_w is the molar mass of water, R is the universal gas constant, and T is the temperature. Model 2 uses equations (1), (2b), and (3) to calculate g(RH). The hygroscopic growth predictions of *Hämeri et al.* [2001, Figure 1] and *Russell and Ming* [2002, Figure 10] are similar to those of model 2.

[11] Dry NaCl particles are not spherical but instead have a cubic shape (cf. images by *Wise et al.* [2005]). Model 3 expands on model 2 by including a correction for the change in particle shape from cubic dry particles to spherical aqueous droplets upon deliquescence. The standard shape factor χ of 1.08 for cubic particles is employed. The relation of $d_{m,dry}$ to $d_{ve,dry}$ to obtain the analog of equation (2b) for model 3 is given by:

$$\chi \frac{d_{ve,dry}}{C_c\left(\mathrm{Kn}\left(\lambda, d_{ve,dry}\right)\right)} = \frac{d_{m,dry}}{C_c\left(\mathrm{Kn}\left(\lambda, d_{m,dry}\right)\right)}, \tag{4}$$

where C_c is the Cunningham slip correction. Model 3 uses equations (1), (2a), (3), and (4) to calculate g(RH).

[12] Model 4 expands on model 3 by including a size-dependent shape factor [*Dahneke*, 1973; *DeCarlo et al.*, 2004]. In the continuum regime of Kn < 0.1, the shape factor χ_c^{cube} of a cubic particle is 1.08. In the free-molecule regime of Kn > 10, however, the shape factor χ_{fm}^{cube} changes to 1.24. In the transition regime of 0.1 < Kn < 10, the size-dependent shape factor χ_t^{cube} (λ, $d_{ve,dry}$; χ_c^{cube}, χ_{fm}^{cube}) is interpolated as follows:

$$\chi_t^{cube} = \chi_c^{cube} \frac{C_c\left(\mathrm{Kn}\left(\lambda, d_{ve,dry}\right)\right)}{C_c\left(\mathrm{Kn}\left(\lambda, \left(\chi_{fm}^{cube}/\chi_c^{cube}\right) d_{ve,dry}\right)\right)}. \tag{5}$$

[1]Auxiliary material is available at ftp://ftp.agu.org/apend/gl/2005gl025199.

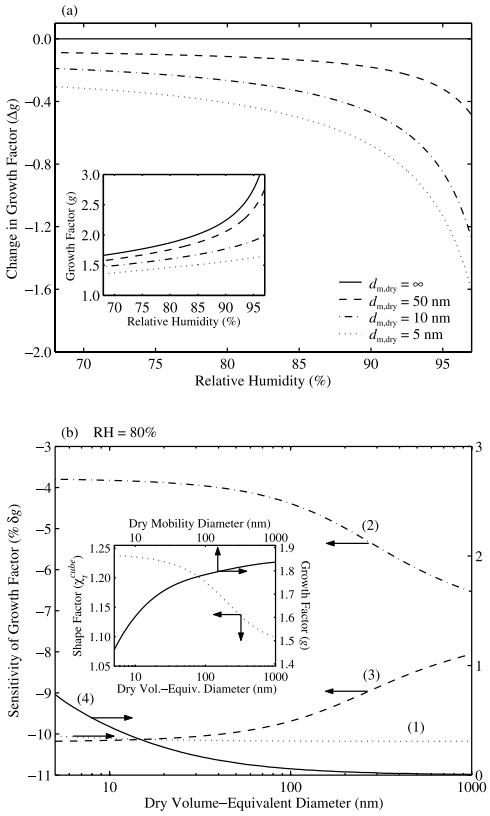

Figure 1. (a) The change in the growth factor of particles having dry-mobility diameters of 5, 10, and 50 nm compared to an infinitely large particle. Inset: growth factor of model 4. (b) The size-dependent sensitivity of the growth factor at 80% RH to (1) the density ρ_s of the dry particle, (2, 3) the shape factor χ of the dry particle, and (4) the surface tension σ_{aq} of the aqueous droplet. Parameters are varied in the sensitivity analysis as follows: (1) ρ_s = 2185, (2) χ = 1.08, (3) $\chi = \chi_t^{cube}$, and (4) $\sigma_{aq} = \sigma_{aq,ref} - 0.004$. The reference condition used for each line is model 2 (see text). (Although the sensitivity analysis varies ρ_s, the difference $(\rho_s - \rho_{aq})$ determines the density-related nanosize effect on growth factor.) Inset: dependence at 1 atm of the shape factor χ_t^{cube} on volume-equivalent diameter (bottom and left axis); dependence for model 4 of the growth factor at 80% RH on dry mobility diameter (top and right axis).

A plot of χ_t^{cube} ($d_{ve,dry}$) at 1 atm is shown in the inset of Figure 1b. The figure shows that χ^{cube} varies from 1.24 for 5-nm particles to 1.10 for 1000-nm particles. Model 4 calculates the simultaneous solution of equations (1), (2a), (3), (4), and (5) to predict g(RH).

[13] An analysis with model 4 shows the dependence of g(RH) on NaCl particle diameter (Figure 1a) and the sensitivity of g(RH) to potential uncertainties in the physical parameters σ_{aq}, χ, and ρ_s (Figure 1b). The inset in Figure 1a shows that g(RH) decreases significantly for particles having dry mobility diameters of 5 to 50 nm, compared to infinitely large particles. The change in growth factor, given as $\Delta g(\mathrm{RH}; d_{m,dry}) = g(\mathrm{RH}; d_{m,dry}) - g(\mathrm{RH}; \infty)$, is shown in Figure 1a. A nanosize effect decreases g(RH) most significantly at high relative humidity. The nanosize effect for fixed RH is shown in the inset of Figure 1b as the plot of

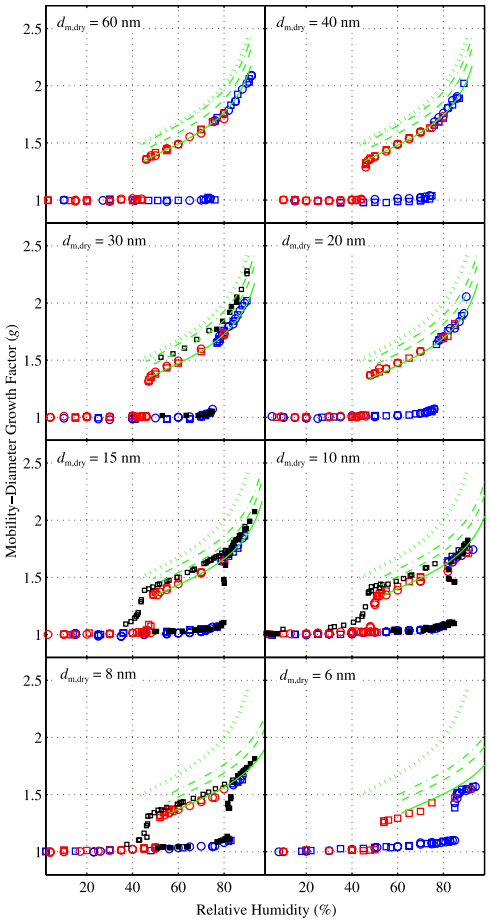

Figure 2. Mobility-diameter growth factors of NaCl nanoparticles. Experimental growth factors are shown by the data points (equation (1)): (open circles) particles generated by electrospray and (open squares) particles generated by vaporization-condensation. Red points are recorded during efflorescence-mode experiments, and blue points are recorded during deliquescence-mode experiments. Black squares show the data of *Hämeri et al.* [2001] for particles generated by atomization. Lines show the growth factors of four models (see §10): model 1 (hatched line), model 2 (dot-dashed line), model 3 (dashed line), and model 4 (solid line). Models are evaluated for $0 < w_t < 45\%$.

$g(80\%)$ from 5 to 1000 nm. The growth factor drops from 1.84 for an infinitely large particle to 1.46 for a particle of 5-nm mobility diameter.

3. Observations of the Nanosize Effect on the Hygroscopic Growth Factor

[14] Hygroscopic growth factors of NaCl nanoparticles were measured both for increasing and for decreasing relative humidity (i.e., "deliquescence-mode" and "efflorescence-mode" experiments, respectively). Details of the experimental apparatus were given by *Biskos et al.* [2006]. Aerosol nanoparticles were generated using two independent methods, namely by vaporizing and condensing granular NaCl and by electrospraying a high-purity NaCl aqueous solution. Nanoparticles are especially susceptible to significant impurities because of their small mass, and self-consistent results from redundant sources are an important test for ruling out the influence of chemical impurities in the observations.

[15] The hygroscopic growth curves for the particles generated by the two methods and for both deliquescence- and efflorescence-mode experiments are the same within measurement uncertainties (Figure 2). In agreement with the predictions of Figure 1, the observations show that the hygroscopic growth of NaCl nanoparticles decreases with decreasing particle size. For example, the mobility-diameter growth factor of 6-nm particles at 80% RH is approximately 1.55 compared to 1.75 for 60-nm particles. The decrease in the growth factor is observed for particle sizes smaller than 40 nm.

[16] The predictions of models 1 to 4 are shown as lines in Figure 2. The measurements agree best with model 4, suggesting that the inclusion of a size-dependent shape factor is critical when interpreting or predicting growth factors of nonspherical nanoparticles. Moreover, model 4 predicts the observations within experimental uncertainties of 2% for RH and 1% for mobility diameter. Therefore, the physical parameters of σ_{aq}, ρ_{aq}, ρ_s, a_w, and χ are known accurately enough to predict nanosize behavior, thus implying no observable size dependence of σ_{aq}, ρ_{aq}, or ρ_s for the nanosizes investigated. The sole exception is that the growth factor of 6-nm particles (the smallest size studied) deviates in a statistically significant way from the predictions of model 4. Either nanosize effects on σ_{aq}, ρ_{aq}, or ρ_s or uncertainties in σ_{aq}, ρ_{aq}, ρ_s, a_w, or χ therefore become quantitatively important at approximately 6 nm. Measurements at even smaller sizes would be highly warranted to expand on this finding.

[17] *Hämeri et al.* [2001] also carried out measurements of the hygroscopic growth of NaCl nanoparticles. Those results are included in Figure 2 as black squares. The two studies have excellent qualitative agreement. There are, however, some nonnegligible differences both in the magnitude of the growth factors (approximately 0.05 higher for *Hämeri et al.* [2001] at lower RH values) and on the promptness of the phase transitions at efflorescence and deliquescence. The measurements of the current study suggest that deliquescence and efflorescence are prompt when a critical RH is passed, whereas the measurements of *Hämeri et al.* [2001] show a nonprompt response, which is more evident for the smaller particle sizes.

[18] A credible explanation of the nonpromptness of particle deliquescence and efflorescence observed by *Hämeri et al.* [2001] is the presence of hygroscopic impurities in the nanoparticles. Precipitation nanoparticles generated by atomizing an aqueous solution (i.e., the method used by *Hämeri et al.* [2001]) may concentrate impurities because the sizes of the primary aqueous droplets prior to evaporation are large [*Kinney et al.*, 1991]. Although little is known about the nature of the impurities, mixed particles have an initial deliquescence relative humidity (DRH) at the eutonic and a final DRH at full solution, i.e., apparant nonprompt deliquescence [*Martin*, 2000]. Moreover, the efflorescence relative humidity (ERH) can decrease if the impurities inhibit critical germ formation.

[19] The level of impurities is lower when a solution is electrosprayed (one of the methods used in this study) rather

than atomized. The primary aqueous droplets are much smaller [*Chen et al.*, 1995]; therefore, they concentrate impurities to a lesser extent in the dry particles. In comparison, the vaporization-condensation technique is an approach for generating NaCl nanoparticles having even smaller levels of impurities. The consistency of the results, both of the DRH and ERH values reported by *Biskos et al.* [2006] and of the growth factors reported herein for particles generated by electrospray or vaporization-condensation, indicates an absence of significant impurities. Several intermediate growth factors apparent in Figure 2 near the ERH arise from small RH differences between the aerosol sample and the sheath air entering the DMA column. The slight increase in the growth factor from 60 to 80% RH is attributed to water adsorption [*Romakkaniemi et al.*, 2001].

4. Conclusions

[20] The hygroscopic growth factors of NaCl particles decrease detectably for sizes below 40 nm across the RH range studied. The growth factors can be accurately predicted by a model that includes the Kelvin effect and a size-dependent shape factor. This factor is derived from first principles [*Dahneke*, 1973] and requires no tuning to the data. An alternative approach of adjusting the dry particle density to fit the observations, as proposed by *Hämeri et al.* [2001], is not necessary. The use of a continuum-regime shape factor instead of a size-dependent shape factor also quantitatively rationalizes the differences between the calculations and the measurements of *Krämer et al.* [2000] and *Gysel et al.* [2002] for 100-nm particles. The good agreement of the predictions of model 4 with the observations also suggests that the aqueous-particle surface tension and density and the dry-particle density are not perceptibly changed from their large-particle values for 8-nm sizes and above. The onset of nanosize effects is, however, suggested by the data for 6-nm particles. Further study is warranted in this regard.

[21] **Acknowledgment.** This material is based upon work supported by the National Science Foundation under Grant 0304213.

References

Anastasio, C., and S. T. Martin (2001), Atmospheric nanoparticles, *Rev. Mineral. Geochem.*, *44*, 293–349.

Biskos, G., A. Malinowski, L. M. Russell, P. R. Buseck, and S. T. Martin (2006), Nanosize effect on the deliquescence and the efflorescence of sodium chloride particles, *Aerosol Sci. Technol.*, *40*, 97–106.

Chen, D.-R., D. Y. H. Pui, and S. L. Kaufman (1995), Electrospraying of conducting liquids for monodisperse aerosol generation in the 4 nm to 1.8 μm diameter range, *J. Aerosol Sci.*, *26*, 963–977.

Chen, J.-P. (1994), Theory of deliquescence and modified Köhler theory, *J. Atmos. Sci.*, *51*, 3505–3516.

Cheng, B., J. Kong, J. Luo, and Y. Dong (1993), Relation of structure stability and Debye temperature to crystal size of nanometer sized TiO_2 powders (in Chinese), *Mater., Sci. Prog.*, *7*, 240–243.

Clarke, A., V. Kapustin, S. Howell, K. Moore, B. Lienert, S. Masonis, T. Anderson, and D. Covert (2003), Sea-salt size distributions from breaking waves: Implications for marine aerosol production and optical extinction measurements during SEAS, *J. Atmos. Oceanic Technol.*, *20*, 1362–1374.

Dahneke, B. E. (1973), Slip correction factors for nonspherical bodies. III, The form of the general law, *J. Aerosol Sci.*, *4*, 163–170.

DeCarlo, P. F., J. G. Slowik, D. R. Worsnop, P. Davidovits, and J. L. Jimenez (2004), Particle morphology and density characterization by combined mobility and aerodynamic diameter measurements. Part 1: Theory, *Aerosol Sci. Technol.*, *38*, 1185–1205.

Djikaev, Y. S., R. Bowles, H. Reiss, K. Hämeri, and A. Laaksonen (2001), Theory of size dependent deliquescence of nanoparticles: Relation to heterogeneous nucleation and comparison with experiments, *J. Phys. Chem. B*, *105*, 7708–7722.

Gilbert, B., F. Huang, H. Zhang, G. A. Waychunas, and J. F. Banfield (2004), Nanoparticles: Strained and stiff, *Science*, *30*, 651–654.

Gysel, M., E. Weingartner, and U. Baltensperger (2002), Hygroscopicity of aerosol particles at low temperatures. 2. Theoretical and experimental hygroscopic properties of laboratory generated aerosols, *Environ. Sci. Technol.*, *36*, 63–68.

Hämeri, K., M. Väkevä, H.-C. Hanson, and A. Laaksonen (2000), Hygroscopic growth of ultrafine ammonium sulphate aerosol measured using an ultrafine tandem differential mobility analyzer, *J. Geophys. Res.*, *105*, 22,231–22,242.

Hämeri, K., A. Laaksonen, M. Väkevä, and T. Suni (2001), Hygroscopic growth of ultrafine sodium chloride particles, *J. Geophys. Res.*, *106*, 20,749–20,757.

Kinney, P. D., D. Y. H. Pui, G. W. Mulholland, and N. P. Bryner (1991), Use of the electrostatic classification method to size 0.1 μm SRM particles—A feasibility study, *J. Res. Natl. Inst. Stand. Technol.*, *96*, 147–176.

Krämer, L., U. Pöschl, and R. Niessner (2000), Microstructural rearrangement of sodium chloride condensation aerosol particles on interaction with water vapor, *J. Aerosol Sci.*, *31*, 673–685.

Lu, H. M., and Q. Jiang (2005), Size-dependent surface tension and Tolman's length of droplets, *Langmuir*, *21*, 779–781.

Martin, S. T. (2000), Phase transitions of aqueous atmospheric particles, *Chem. Rev.*, *100*, 3403–3453.

O'Dowd, C. D., J. L. Jimenez, R. Bahreini, R. C. Flagan, J. H. Seinfeld, K. Hämeri, L. Pirjola, M. Kulmala, S. G. Jennings, and T. Hoffmann (2002a), Marine aerosol formation from biogenic iodine emissions, *Nature*, *417*, 632–636.

O'Dowd, C. D., P. Aalto, K. Hämeri, M. Kulmala, and T. Hoffmann (2002b), Aerosol formation—Atmospheric particles from organic vapours, *Nature*, *416*, 497–498.

Romakkaniemi, S., K. Hämeri, M. Väkevä, and A. Laaksonen (2001), Adsorption of water on 8–15 nm NaCl and $(NH_4)_2SO_4$ aerosols measured using an ultrafine tandem differential mobility analyzer, *J. Phys. Chem. A*, *105*, 8183–8188.

Russell, L. M., and Y. Ming (2002), Deliquescence of small particles, *J. Chem. Phys.*, *116*, 311–321.

Russell, L. M., et al. (1999), Aerosol dynamics in ship tracks, *J. Geophys. Res.*, *104*, 31,077–31,096.

Tang, I. N., A. C. Tridico, and K. H. Fung (1997), Thermodynamic and optical properties of sea salt aerosols, *J. Geophys. Res.*, *102*, 23,269–23,275.

Wise, M. E., G. Biskos, S. T. Martin, L. M. Russell, and P. R. Buseck (2005), Aerosol phase transitions studied using a transmission electron microscope with an environmental cell, *Aerosol Sci. Technol.*, *39*, 849–856.

Zhang, Q., C. O. Stanier, M. R. Canagaratna, J. T. Jayne, D. R. Wornsnop, S. N. Pandis, and J. L. Jimenez (2004), Insights into the chemistry of new particle formation and growth events in Pittsburgh based on aerosol mass spectrometry, *Environ. Sci. Technol.*, *38*, 4797–4809.

G. Biskos and S. T. Martin, Division of Engineering and Applied Sciences, Harvard University, Cambridge, MA 02138, USA. (corresponding author: scot_martin@harvard.edu)

P. R. Buseck, Departments of Geological Sciences and Chemistry/Biochemistry, Arizona State University, Tempe, AZ 85287, USA.

L. M. Russell, Scripps Institution of Oceanography, University of California, San Diego, La Jolla, CA 92093, USA.